


# When gravitational decoupling and quantum gravity (re)unite

R. Casadio 

*Dipartimento di Fisica e Astronomia, Università di Bologna,  
via Irnerio 46, 40126 Bologna, Italy and  
I.N.F.N., Sezione di Bologna, I.S. FLAG,  
viale B. Pichat 6/2, 40127 Bologna, Italy\**

I. Kuntz 

*Departamento de Física, Universidade Federal do Paraná,  
PO Box 19044, Curitiba – PR, 81531-980, Brazil.†*

R. da Rocha 

*Federal University of ABC, Center of Mathematics, Santo André, 09210-580, Brazil.‡*

The effective action for quantum gravity coupled to matter contains corrections arising from the functional measure. We analyse the effect of such corrections for anisotropic self-gravitating compact objects described by means of the gravitational decoupling method applied to isotropic solutions of the Einstein field equations. In particular, we consider the Tolman IV solution of general relativity and show that quantum gravity effects can modify the effective energy density as well as the effective tangential and radial pressures. For a suitable choice of the mimicking constant, upper bounds on the quantum corrections can be driven by the surface redshift of the anisotropic compact stellar system obtained with the gravitational decoupling.

## I. INTRODUCTION

The experimental detection of gravitational waves radiated from the final stages of binary mergers [1] has opened a window into the strong gravity regime. Solutions of the Einstein field equations and their generalisations can therefore be experimentally tested. The gravitational decoupling (GD) of the Einstein equations is a method for obtaining self-gravitating compact stellar configurations starting from known solutions of general relativity (GR). Anisotropic stars arise in a very natural way in the GD approach, yielding the possibility of obtaining analytical solutions to the Einstein

---

\*Electronic address: [casadio@bo.infn.it](mailto:casadio@bo.infn.it)

†Electronic address: [kuntz@fisica.ufpr.br](mailto:kuntz@fisica.ufpr.br)

‡Electronic address: [roldao.rocha@ufabc.edu.br](mailto:roldao.rocha@ufabc.edu.br)

field equations supplemented by general forms of the energy-momentum tensor [2–4]. The GD includes, as a particular case, the minimal geometrical deformation (MGD) [5, 6], which was originally formulated in order to describe compact stars and black holes in the brane-world [7–9], including soft hair [10].

In the GD method, sources of the GR gravitational field and the corresponding field equations are split into two parts. The first one describes a GR solution, whereas the second part contains additional sources, which can carry any type of charge, including tidal and gauge ones, hairy fields of any physical origin, as well as any other contributions from extended models of gravity. Examples of configurations so obtained can be found in Refs. [11–30]. Realistic models based on relativistic description of nuclear interactions suggest that star interiors are anisotropic at extremely high densities. The GD method easily allows for including pressure anisotropies [31–50]. The MGD applies naturally in the AdS/CFT scenario [51–53] for studying black holes with physically viable low-energy limits [54, 55]. The trace and Weyl anomalies were also calculated for hairy GD solutions, establishing new possibilities of employing the AdS/CFT to the membrane paradigm [56, 57]. Quasinormal modes radiated from hairy GD solutions were also addressed recently in Ref. [58–62].

In the functional approach to quantum gravity, a functional measure is required for obtaining an effective action which remains invariant under field redefinitions (hence gauge transformations, see [63] and references therein). This approach was employed in previous works to study the spacetime stability [64] as well as the weakly-coupled gravity and the strongly-coupled conformal field theory sides of the gauge/gravity correspondence [65]. Corrections to transport and response coefficients in relativistic second-order hydrodynamics were obtained using the linear response procedure. The shear viscosity, entropy density, diffusion constant, and speed of sound, were shown not to achieve any corrections from the functional measure of gravity. On the other hand, the energy density, pressure, relaxation time, shear relaxation, bulk viscosity, decay rate of sound waves, and coefficients of conformal traceless tensor fields, were shown to carry significant quantum corrections due to the functional measure, also reflecting the instability of the strongly-coupled fluids on the boundary CFT. This opens up the possibility of testing quantum gravity with the quark-gluon plasma, as neutron stars can contain hadronic and quark phases. Analogously to asymptotic freedom, which permits matter deconfinement when the density increases at low temperatures, this kind of phenomenon could naturally occur in the inner core of neutron stars and quark stars [66–68].

The main goal of this paper is to study the effects of the contribution from the functional measure in the effective action for anisotropic stellar configurations obtained with the GD method in general. In particular, we will then consider the MGD of the Tolman IV solution found in Ref. [4]

to include quantum gravity effects analysed in Ref. [69].

We will deal with complex metric functions by simply considering their modulus and the Kontsevich–Segal (KS) condition that complex metrics should satisfy in order to represent acceptable backgrounds for quantum field theory (QFT) [70]. In particular, the KS theorem states that the sum of the modulus of the arguments of the eigenvalues of a complex metric must be less than  $\pi$ , which we will take as a criterion hereby. We will show that instabilities generated by the functional measure can be cancelled and the metric components remain real in the interior of the stellar distribution for some choice of the mimic constraint. However, the effective energy density still carries instabilities of the degrees of freedom in the fluid, and the effective tangential and radial pressures are affected by quantum gravity effects. For another choice of the mimic constraint, the ADM mass, the effective radial and tangential pressures as well as the energy densities carry effects of both the GD hairy charge and the parameter regulating quantum gravity effects.

The paper is organized as follows: in Section II the functional measure is introduced in quantum field theory (QFT), playing an important role in the construction of the configuration-space metric, contributing to an additional expression in the effective action of quantum gravity corresponding to 1-loop corrections. Section III is devoted to briefly reviewing the GD setup and analyzing modifications due to the functional measure. Compact self-gravitating stellar systems are scrutinized in this context. Section IV addresses the GD of Tolman IV solutions with quantum gravity corrections. The surface redshift bounds are then used to constrain the maximum magnitude of the parameter governing quantum gravity effects. Section V presents some concluding remarks and future perspectives. Appendixes (A 1, A 2) present other choices of the mimicking constraints and subsequent analyses.

## II. FUNCTIONAL MEASURE IN QUANTUM FIELD THEORY

Despite the wide applicability of path integrals in physics, a well-defined mathematical construction, and whether it can be indeed interpreted as an integral, remains unknown. To a great extent, the problem boils down to the definition of the functional measure. The issue has been studied since long and different definitions have been suggested [71–79]. Although still quite formal, such manipulations could have phenomenological consequences that have largely been dismissed by the use of dimensional regularization, where the measure is regularized to unity.

Dimensional regularization is indeed the most prominent form of regularization used nowadays when dealing with field theories in the continuum. It has several advantages, including the ease-

of-use and preservation of symmetries at every step of the calculation [80]. However, applying dimensional regularization to the functional measure only hides the issue. Anomalies, for example, result from the non-invariance of the functional measure, which could have never been observed if dimensional regularization were adopted in the path integral.

Other forms of regularization, such as cutoff and lattice, forces one to deal with all aspects of the functional measure. In particular, in the absence of a rigorous definition of the path integral, its interpretation relies on the continuum limit of a lattice. This procedure-based approach, albeit ambiguous, is the only known way of giving meaning to the Feynman integrals and necessarily requires understanding of the functional measure. The existence of physical cutoffs, as implemented in Wilson's effective theory [81] and envisaged in minimal length scenarios [82–84], is yet another reason that calls for a better understanding of the integration measure.

From a geometrical perspective, invariance under all of the underlying symmetries is obtained from the generating functional

$$Z[J] = \int d\mu[\varphi] e^{\frac{i}{\hbar}(S[\varphi]+J_i \varphi^i)} , \quad (1)$$

where  $S[\varphi]$  is the bare action,  $\varphi^i = (\phi(x), A_\mu(x), g_{\mu\nu}(x), \dots)$  denotes a set of fields (formally) sourced by the external currents  $J_i$ , and

$$d\mu[\varphi] = \prod_i d\varphi^i \sqrt{\text{Det}G_{jk}(\varphi)} , \quad (2)$$

is the functional measure.  $\text{Det}G_{ij}(\varphi)$  denotes the functional determinant of the field configuration-space metric  $G_{ij}$ . The factor  $\sqrt{\text{Det}G_{ij}}$  must be included to cancel the Jacobian from  $\prod_i d\varphi^i$ , thus leaving the total measure  $d\mu[\varphi]$  invariant under field redefinitions. One should note that such a factor is required even for a flat configuration space, because the Jacobian of general field transformations is not one. Using the relation  $\text{Det} \log = \log \text{Tr}$ , we can write

$$\text{Det}G_{ij} = e^{\int d^4x \sqrt{-g} \text{tr} \log G_{IJ}} , \quad (3)$$

where  $g$  is the determinant of the spacetime metric  $g_{\mu\nu}$  and we used the functional trace

$$\text{Tr} A_{ij} = \int d^4x \sqrt{-g} \text{tr} A_{IJ}(x, x) , \quad (4)$$

including summation over discrete indices ( $I, J$ ), via the ordinary trace  $\text{tr}$ , and integration over spacetime. From Eqs. (1) and (3), one then finds

$$Z[J] = \int \prod_i d\varphi^i e^{\frac{i}{\hbar}(S_{\text{eff}}[\varphi]+J_j \varphi^j)} , \quad (5)$$

where we defined the Wilsonian effective action <sup>1</sup>

$$S_G = \int d^4x \sqrt{-g} \left( \mathcal{L} - \frac{i}{2} \hbar \operatorname{tr} \log G_{IJ} \right) , \quad (6)$$

for some bare Lagrangian  $\mathcal{L}$  corresponding to the bare action  $S$ .

The configuration-space metric must be seen as part of the definition of the theory, hence physical systems are now fully described by the pair  $(S[\varphi], G_{ij})$ . The sole specification of the classical action can no longer secure uniqueness, with different  $G_{ij}$  representing different quantization schemes. The determination of  $G_{ij}$  follows closely the procedure to obtain the action. As often done, we shall assume ultralocality, namely

$$G_{ij} = G_{IJ}(\varphi) \delta^{(4)}(x, x') , \quad (7)$$

and some symmetry principles to fix  $G_{IJ}(\varphi)$ . Note that  $G_{IJ}(\varphi)$  is a function (not functional) of the fields which describes the metric of the finite-dimensional space obtained by fixing the spacetime point. The form of the configuration-space metric in Eq. (7) guarantees the same  $G_{IJ}$  across all spacetime points and prevents interactions from distant events.

From a physical viewpoint, there is nothing fundamental about ultralocality. One could as well have assumed locality instead, in which case there would appear terms with derivatives of the Dirac delta in Eq. (7). Ultralocality is a working assumption, allowing one to make sense of the functional logarithm as the continuum extension of the logarithm of a direct sum,

$$\log \left[ G_{IJ} \delta^{(4)}(x, x') \right] = \log(G_{IJ}) \delta^{(4)}(x, x') . \quad (8)$$

However, ultralocality causes the appearance of  $\delta^{(4)}(0)$  in spacetime integrations, as can be seen from Eqs. (4) and (8). Replacing dimensional regularization in favour of other regulators is a way to explore functional measure effects without facing the difficulties introduced by trading ultralocality for the locality.

We shall here adopt a Gaussian regularization

$$\delta^{(4)}(x) \rightarrow \frac{e^{-\frac{x^2}{2L_{UV}^2}}}{(2\pi)^2 L_{UV}^4} , \quad (9)$$

where  $K_{UV} = \hbar/L_{UV}$  is a Wilsonian UV cutoff. In studying compact objects of mass  $M$  and size  $R_s$ , we shall be typically interested in configurations with energy densities  $\rho \sim M/R_s^3 \ll m_p/\ell_p^3$ , where

---

<sup>1</sup> It is clear that the contribution from the functional measure is of the same order (in  $\hbar$ ) as 1-loop corrections which we will discuss later.

$m_p$  is the Planck mass and  $\ell_p$  the Planck length.<sup>2</sup> We can therefore assume  $\rho \ll \hbar/L_{UV}^4 \ll m_p/\ell_p^3$  (or, typically,  $\ell_p \ll L_{UV} \ll R$ ). This way, we obtain

$$S_\mu = \int d^4x \sqrt{-g} (\mathcal{L} - i\zeta \operatorname{tr} \log G_{IJ}) , \quad (10)$$

where  $\zeta = \zeta(K_{UV}) \propto \hbar/L_{UV}^4$  is a Wilsonian coefficient whose running is such that

$$K_{UV} \frac{dZ[J]}{dK_{UV}} = 0 . \quad (11)$$

Note that the correction due to the measure scales quartically with the cutoff  $K_{UV}$ , thus  $\operatorname{tr} \log G_{IJ}$  is a relevant operator and  $\zeta$  is UV sensitive.

Beside the functional measure discussed above, after performing the path integral in Eq. (1) at the 1-loop level, the effective action also gains contribution from the Hessian

$$\Gamma[\varphi] = S_G[\varphi] + \frac{i}{2} \hbar \operatorname{Tr} \log \mathcal{H}_{ij} . \quad (12)$$

Note that, individually, the corrections in Eqs. (10) and (12) do not transform covariantly, because the determinant of a 2-rank tensor is basis-dependent. Their combination however results in

$$\operatorname{Tr} \log \left( G^{ik} \mathcal{H}_{kj} \right) = \operatorname{Tr} \log \mathcal{H}^i_j , \quad (13)$$

which is invariant and shows the important role played by the functional measure.

### A. Effective action for gravity and matter

For pure gravity, one has  $\varphi^i = g^{\mu\nu}(x)$  and  $i = (\mu\nu, x)$ . To lowest order, one then finds the DeWitt metric  $G_{IJ} = G_{\mu\nu\rho\sigma}$ , where<sup>3</sup>

$$G_{\mu\nu\rho\sigma} = \frac{1}{2} (g_{\mu\rho} g_{\nu\sigma} + g_{\mu\sigma} g_{\nu\rho} - a g_{\mu\nu} g_{\rho\sigma}) \quad (14)$$

and  $a$  is a dimensionless parameter.

When matter is present, there could be other contributions to  $G_{IJ}$ . For example, for a scalar field coupled to gravity  $\varphi^i = (g_{\mu\nu}(x), \phi(x))$ , the simplest non-trivial choice for the field-space metric would read [85, 86]

$$G_{IJ} = \begin{pmatrix} G_{\phi\phi} & 0 \\ 0 & G_{\mu\nu\rho\sigma} \end{pmatrix} , \quad (15)$$

<sup>2</sup> In units with the speed of light  $c = 1$ , the (reduced) Planck mass and length are given by  $G_N = \ell_p/m_p$  and  $\hbar = m_p \ell_p$ . In the following, we shall also use  $\kappa = 8\pi G_N$  and the spacetime signature  $(-+++)$ .

<sup>3</sup> In principle, Eq. (14) could be multiplied by a global factor  $g^\epsilon = (\det g_{\mu\nu})^\epsilon$ . We take  $\epsilon = 0$  for simplicity.

where

$$G_{\phi\phi} = c_1 + c_2 L_{\text{UV}} \frac{\phi}{\sqrt{\hbar}} , \quad (16)$$

and  $c_i$  are free dimensionless parameters. Since

$$\det G_{IJ} = (\det G_{\phi\phi}) (\det G_{\mu\nu\rho\sigma}) , \quad (17)$$

the measure term in Eq. (12) splits into matter and gravity contributions

$$\text{Tr} \log G_{ij} = \zeta \int d^4x \sqrt{-g} \left[ \log \left( c_1 + c_2 L_{\text{UV}} \frac{\phi}{\sqrt{\hbar}} \right) + \text{tr} \log G_{\mu\nu\rho\sigma} \right] . \quad (18)$$

We have here determined  $G_{\phi\phi}$  in the spirit of effective field theory by implementing an expansion in the energy (density). However, a fundamental measure could in principle be any function  $f(\phi)$  of the scalar field, and we shall take advantage of this feature in the following.

We shall take the bare Lagrangian for GR minimally coupled to matter, namely

$$\mathcal{L} = \frac{R}{2\kappa} + \mathcal{L}_m(\phi) , \quad (19)$$

where  $R$  is the Ricci scalar and  $\mathcal{L}_m$  is the Lagrangian for the scalar field. Then the Hessian reads

$$\mathcal{H}_{\mu\nu\rho\sigma} = K_{\mu\nu\rho\sigma} \square + U_{\mu\nu\rho\sigma} , \quad (20)$$

where

$$K_{\mu\nu\rho\sigma} = \frac{1}{4} (g_{\mu\rho} g_{\nu\sigma} + g_{\mu\sigma} g_{\nu\rho} - g_{\mu\nu} g_{\rho\sigma}) \quad (21)$$

and  $U_{\mu\nu\rho\sigma}$  is a tensor that depends on the spacetime curvature, whose form is not important. From Eqs. (14) and (20), we can write (13) as [69]

$$\begin{aligned} \text{Tr} \log \mathcal{H}^i_j = & -\zeta \int d^4x \sqrt{-g} \left\{ \log \left( c_1 + c_2 L_{\text{UV}} \frac{\phi}{\sqrt{\hbar}} \right) - \log \det \left[ \frac{1}{2} \left( \delta_{(\mu}^{\rho} \delta_{\nu)}^{\sigma} + (a-1) g_{\mu\nu} g^{\rho\sigma} \right) \right] \right. \\ & \left. - \log \det \left[ \delta_{(\alpha}^{\mu} \delta_{\beta)}^{\nu} \square + (K^{-1})^{\mu\nu\rho\sigma} U_{\rho\sigma\alpha\beta} \right] \right\} , \quad (22) \end{aligned}$$

where we pulled out  $K_{\mu\nu\rho\sigma}$  from  $H_{\mu\nu\rho\sigma}$  and put it along with  $G_{\mu\nu\rho\sigma}$ . The last term in Eq. (22) can be obtained as a power series in the curvature or derivatives [87–89]. Such a term represents next-to-leading order contributions when compared to the second term in Eq. (22), which contains no derivatives, thus we can safely drop it at low energies. Finally, the matrix determinant lemma yields the effective action

$$\Gamma[g] = \int d^4x \sqrt{-g} \left[ \frac{R}{2\kappa} + \mathcal{L}_m + i \frac{\zeta}{2} \log \left( \frac{4a-3}{256} \right) - i \frac{\zeta}{2} \log \left( c_1 + c_2 L_{\text{UV}} \frac{\phi}{\sqrt{\hbar}} \right) \right] , \quad (23)$$

which depends on the parameters  $\zeta \sim K_{\text{UV}}^4$ ,  $a$  and  $c_i$ , and on the (expectation value of the) scalar (matter) field in the configurations of interest.

## B. Effective field equations for compact objects

We observe that the term associated with the quantum measure for gravity in Eq. (23) is constant and would therefore be the same inside as well as in the vacuum outside a compact matter source. It is therefore safe to assume that it is negligibly small, which is achieved for  $a \simeq 259/4$ .

The second correction depends on the (expectation value of the) scalar field, or more generally on a (smooth) function of (the expectation value of)  $\phi$ , and we may also assume that it is negligible in the vacuum where  $\phi \simeq 0$ . This implies that  $c_1 \simeq 1$ .

Moreover, in order to consider more general forms of matter than just a scalar field, we notice that  $\phi \sim \rho$ , the (proper) energy density inside a compact object. We can therefore write the effective field equations as

$$R_{\mu\nu} - \frac{1}{2} R g_{\mu\nu} = \kappa T_{\mu\nu} - i \kappa \frac{\zeta}{2} \log\left(1 + \frac{\rho}{\Upsilon}\right) g_{\mu\nu} , \quad (24)$$

where  $T_{\mu\nu}$  is the energy-momentum tensor derived from the matter Lagrangian  $\mathcal{L}_m$  and  $\Upsilon$  is an energy density associated with the UV cutoff  $K_{UV}$  of the effective theory. Clearly, GR is smoothly recovered in the limit  $\zeta \rightarrow 0$ , as well as for  $\Upsilon \rightarrow \infty$ . In fact, given that the effective action (23) holds in the regime in which  $\rho \ll \Upsilon$ , we can further expand the quantum correction and obtain

$$R_{\mu\nu} - \frac{1}{2} R g_{\mu\nu} \simeq \kappa T_{\mu\nu} - i \kappa \bar{\zeta} \rho g_{\mu\nu} , \quad (25)$$

where  $\bar{\zeta} \simeq \zeta/2\Upsilon$  is a dimensionless parameter.

The imaginary contribution in Eq. (25) may yield complex solutions, which requires some comments. Although the Universe is described by a real metric with Lorentzian signature, energy-momentum tensors with an imaginary part and complex metrics have been already considered, for example, in Refs. [90–92]. Gibbons and Hawking [93] showed that the Kerr metric becomes complex-valued, and nondegenerate if the angular momentum is assumed to be real, recovering the predicted thermodynamics underlying the Kerr metric. Later, Gibbons, Hawking, and Perry [94] stated that the path integral formalism of quantum gravity must be realized as the infinite-dimensional analogue of a complex contour integration running over complex spacetime metrics, based upon the fact that the action of Euclidean quantum gravity has no positive-definite property. They also showed that complex spacetimes can be employed in QFTs on curved spacetimes and in quantum gravity, studying complex extensions of the Kerr and Schwarzschild metrics. Topological transitions were studied in Ref. [95], with complex spacetime metrics describing tunnelling trajectories. In a semiclassical theory of gravity coupled to matter described by quantum fields, complex metrics



can emerge. Kontsevich and Segal classified the complex metrics in which a generic QFT can be consistently coupled [70], which paved the way for obtaining classes of suitable complex metrics for quantum gravity. The KS theorem establishes a criterion to determine which complex metrics are compatible with the demand that QFTs may be consistently defined, according to a bound on the summation of the arguments of its eigenvalues. Witten showed that the KS criterion can be applied to dynamical gravity [96], by analyzing several complex solutions and showing that the KS theorem selects a relevant set of complex metrics, like complex black holes [97, 98]. Visser [99] recently studied Feynman's  $i\varepsilon$ -prescription for propagators in QFT in terms of complex spacetime metrics, also extending this prescription to QFT both on a fixed background and in a fuzzy spacetime geometry. Besides proposing relevant extensions of the weak energy condition, it implies constraints on the configuration space of admissible off-shell geometries that are consistent with path integrals in quantum gravity [99, 100]. The 2-point correlation function of massive scalar fields can be also evaluated by semiclassical methods. Some spacelike points cannot be connected by real geodesics, however complex geodesics can link these points by analytical continuation to the sphere. Therefore 1-loop corrections to the correlator can be computed in holographic models [101]. Despite the fact that the quantum measure induces an imaginary contribution to the energy-momentum tensor, we will show that such a contribution can be compensated for in the interior region of the compact stellar distribution and the metric remains real, given a particular mimic constraint. Other choices of the mimic constraint yields the metric with a complex radial component. Of course, this comes at the expense of the effective energy density and the radial and tangential pressures.

### III. GRAVITATIONAL DECOUPLING AND FUNCTIONAL MEASURE

We can now add the quantum correction described in the previous Section to solutions obtained by applying the GD method [2] by simply considering the field equations (24) with the matter energy-momentum tensor

$$T_{\mu\nu} = T_{\mu\nu}^{(M)} + \alpha \theta_{\mu\nu} , \quad (26)$$

where

$$T_{\mu\nu}^{(M)} = (\rho + p) u_\mu u_\nu + p g_{\mu\nu} \quad (27)$$

represents the energy-momentum tensor of a perfect fluid with 4-velocity  $u^\mu$ , density  $\rho$ , and isotropic pressure  $p$ . The term  $\theta_{\mu\nu}$  in Eq. (26) corresponds to the contribution of additional sources, as

recalled in the Introduction, and it contains the parameter  $\alpha$  so that the perfect fluid description can be recovered in the limit  $\alpha \rightarrow 0$ . Since the Einstein tensor in the left hand side of Eq. (24) satisfies the Bianchi identity, the energy-momentum tensor (26) must satisfy the conservation equation

$$\nabla_\mu T^{\mu\nu} = i \frac{\zeta}{2} g^{\mu\nu} \nabla_\mu \left[ \log \left( 1 + \frac{\rho}{\Upsilon} \right) \right] \simeq i \bar{\zeta} g^{\mu\nu} \nabla_\mu \rho . \quad (28)$$

A static and spherically symmetric metric can always be written in Schwarzschild-like coordinates as

$$ds^2 = -e^{\nu(r)} dt^2 + e^{\lambda(r)} dr^2 + r^2 d\Omega^2 , \quad (29)$$

where  $\nu = \nu(r)$ ,  $\lambda = \lambda(r)$ , and  $d\Omega^2 = d\theta^2 + \sin^2 \theta d\phi^2$ . The fluid inside the star has 4-velocity with the only non-zero component  $u^0 = e^{-\nu(r)/2}$  in the range  $0 \leq r \leq R_s$ , where  $r = R_s$  corresponds to the stellar surface. The field equations (24) for the metric (29) read

$$\kappa \left[ \rho + i \frac{\zeta}{2} \log \left( 1 + \frac{\rho}{\Upsilon} \right) - \alpha \theta_0^0 \right] = -\frac{1}{r^2} - e^{-\lambda} \left( \frac{1}{r^2} - \frac{\lambda'}{r} \right) \quad (30a)$$

$$\kappa \left[ p - i \frac{\zeta}{2} \log \left( 1 + \frac{\rho}{\Upsilon} \right) + \alpha \theta_1^1 \right] = \frac{1}{r^2} - e^{-\lambda} \left( \frac{1}{r^2} + \frac{\nu'}{r} \right) \quad (30b)$$

$$\kappa \left[ p - i \frac{\zeta}{2} \log \left( 1 + \frac{\rho}{\Upsilon} \right) + \alpha \theta_2^2 \right] = \frac{e^{-\lambda}}{4} \left( \lambda' \nu' + 2 \frac{\nu' - \lambda'}{r} - 2 \nu'' - \nu'^2 \right) , \quad (30c)$$

where primes denote derivatives with respect to the areal radius  $r$  and the conservation equation (28) yields

$$p' + \frac{\nu'}{2} (\rho + p) + \alpha (\theta_1^1)' - \alpha \frac{\nu'}{2} (\theta_0^0 - \theta_1^1) + \frac{2\alpha}{r} (\theta_2^2 - \theta_1^1) = i \frac{\zeta}{2} \frac{\rho'}{\Upsilon + \rho} . \quad (31)$$

From the system (30a)-(30c), one can define the effective density

$$\dot{\rho} = \rho - \alpha \theta_0^0 + i \frac{\zeta}{2} \log \left( 1 + \frac{\rho}{\Upsilon} \right) \simeq \rho - \alpha \theta_0^0 + i \bar{\zeta} \rho , \quad (32)$$

whose imaginary part corresponds to the instability of the fluid and measures the flow lifetime [86]. Also, the effective radial pressure can be read off as

$$\dot{p}_r = p + \alpha \theta_1^1 - i \frac{\zeta}{2} \log \left( 1 + \frac{\rho}{\Upsilon} \right) \simeq p + \alpha \theta_1^1 - i \bar{\zeta} \rho , \quad (33)$$

as well as the effective tangential pressure

$$\dot{p}_t = p + \alpha \theta_2^2 - i \frac{\zeta}{2} \log \left( 1 + \frac{\rho}{\Upsilon} \right) \simeq p + \alpha \theta_2^2 - i \bar{\zeta} \rho . \quad (34)$$

The additional source  $\theta_{\mu\nu}$  induces the anisotropy

$$\Pi(r, \alpha) \equiv \dot{p}_t(r, \alpha) - \dot{p}_r(r, \alpha) = \alpha (\theta_2^2 - \theta_1^1) , \quad (35)$$

which does not depend on the functional measure.

The MGD can be implemented to solve the system (30a)-(31), by considering the specific GR solution for an isotropic fluid described by  $T_{\mu\nu}^{(M)}$  in the limit  $\alpha \rightarrow 0$ , which we write as

$$ds^2 = -e^{\xi(r)} dt^2 + \frac{dr^2}{\mu(r)} + r^2 d\Omega^2 , \quad (36)$$

where

$$\mu(r) \equiv 1 - \frac{\kappa^2}{r} \int_0^r x^2 \rho(x) dx = 1 - \frac{2m(r)}{r} , \quad (37)$$

with  $m$  the Misner-Sharp-Hernandez mass function representing the energy within a sphere of areal radius  $r$ . One can then switch on the parameter  $\alpha$  to include the effects of the source  $\theta_{\mu\nu}$  on the perfect fluid solution. The GD of the metric functions are then given by

$$\xi(r) \mapsto \nu(r) = \xi(r) + \alpha \chi(r) , \quad (38a)$$

$$\mu(r) \mapsto e^{-\lambda(r)} = \mu(r) + \alpha f(r) . \quad (38b)$$

The MGD corresponds to setting  $\chi = 0$  and solving for  $f \equiv f^\diamond$ . The resulting metric is of the form in Eq. (29) with

$$\mu(r) \mapsto e^{-\lambda(r)} = \mu(r) + \alpha f^\diamond(r) , \quad (39)$$

whereas  $e^{\nu(r)}$  is unaltered.

### A. MGD and functional measure

Upon replacing Eq. (39) in the field equations (30a)-(31), the system splits into two sets. In the original (M)GD approach, the first set (corresponding to the limit  $\alpha \rightarrow 0$ ) is solved by the chosen metric (36) by construction and one is left with a set of equations that can be used to determine a consistent configuration of  $f^\diamond$  and  $\theta_{\mu\nu}$ . In the present case, beside  $\theta_{\mu\nu}$ , we have contributions from the functional measure and we include their effects into the second set, which we then solve perturbatively in  $\bar{\zeta} \sim \zeta/\Upsilon$ .

As we just mentioned, the first system of equations corresponds to the standard Einstein field equations for the perfect fluid, that is

$$\kappa \rho = -\frac{1}{r^2} - \frac{\mu}{r^2} - \frac{\mu'}{r} \quad (40a)$$

$$\kappa p = \frac{1}{r^2} + \mu \left( \frac{1}{r^2} + \frac{\nu'}{r} \right) \quad (40b)$$

$$\kappa p = -\frac{\mu}{4} \left( 2\nu'' + \nu'^2 + \frac{2\nu'}{r} \right) + \frac{\mu'}{4} \left( \nu' + \frac{2}{r} \right) , \quad (40c)$$

along with Eq. (31) in the limit  $\alpha \rightarrow 0$ ,

$$p' + \frac{\nu'}{2} (\rho + p) = 0. \quad (41)$$

The second set of equations contains the solution  $\nu$  of the previous Eqs. (40a)-(41), the MGD deformation  $f^\diamond$  and the additional source  $\theta_{\mu\nu}$ , as well as the correction from the quantum measure,

$$\kappa [\theta_0^0 + i \bar{\zeta} \rho] = -\frac{f^\diamond}{r^2} - \frac{f^{\diamond'}}{r} \quad (42a)$$

$$\kappa [\theta_1^1 - i \bar{\zeta} \rho] = f^\diamond \left( \frac{1}{r^2} + \frac{\nu'}{r} \right) \quad (42b)$$

$$\kappa [\theta_2^2 - i \bar{\zeta} \rho] = -\frac{f^\diamond}{4} \left( 2\nu'' + \nu'^2 + \frac{2\nu'}{r} \right) + \frac{f^{\diamond'}}{4} \left( \nu' + \frac{2}{r} \right). \quad (42c)$$

Furthermore,  $\theta_{\mu\nu}$  must satisfy the conservation equation (31) restricted to this sector, to wit

$$(\theta_1^1)' - \frac{\nu'}{2} (\theta_0^0 - \theta_1^1) - \frac{2}{r} (\theta_2^2 - \theta_1^1) = i \frac{\zeta}{2\alpha} \frac{\rho'}{\Upsilon + \rho}. \quad (43)$$

The above implies that there is no direct exchange of energy-momentum between the source  $\theta_{\mu\nu}$  and the perfect fluid, but only with the quantum corrections which are on the same footing as  $\theta_{\mu\nu}$ , so that the interaction between the two sectors is purely gravitational.

As noticed in Ref. [2], the right hand side of Eqs. (42a)-(42c) resemble the standard spherically symmetric field Eqs. (40a)-(40c) for  $\zeta = 0$ , except for the missing  $1/r^2$  terms. This leads us to associate with  $\theta_{\mu\nu}$  the effective energy density  $\hat{\rho}$ , effective radial pressure  $\hat{p}_r$ , and effective tangential pressure  $\hat{p}_t$ , respectively given by

$$\hat{\rho} = -\alpha \theta_0^{\diamond 0} = -\alpha \theta_0^0 - \frac{\alpha}{\kappa r^2} - i \bar{\zeta} \rho, \quad (44a)$$

$$\hat{p}_r = \alpha \theta_1^{\diamond 1} = \alpha \theta_1^1 + \frac{\alpha}{\kappa r^2} + i \bar{\zeta} \rho, \quad (44b)$$

$$\hat{p}_t = \alpha \theta_2^{\diamond 2} = \alpha \theta_2^2 + i \bar{\zeta} \rho = \alpha \theta_3^{\diamond 3} = \alpha \theta_3^3 + i \bar{\zeta} \rho. \quad (44c)$$

Eq. (43) then reads

$$(\theta_1^{\diamond 1})' - \frac{\nu'}{2} (\theta_0^{\diamond 0} - \theta_1^{\diamond 1}) - \frac{2}{r} (\theta_2^{\diamond 2} - \theta_1^{\diamond 1}) = i \frac{\zeta}{\alpha} \frac{\rho'}{\Upsilon + \rho}. \quad (45)$$

Since the conservation Eq. (43) [or (45)] is again a linear combination of the field Eqs. (42a)-(42c), the MGD eventually results in four unknown functions  $f^\diamond$ ,  $\theta_0^0$ ,  $\theta_1^1$ ,  $\theta_2^2$  satisfying Eqs. (42a)-(42c) [or the equivalent anisotropic system (44a)-(44c)].

## B. Compact objects

A spherically symmetric star can be described by a perfect fluid of energy-momentum  $T_{\mu\nu}^{(M)}$  localised within a radius  $r = R_s$ , to which we can add both the (anisotropic) source  $\theta_{\mu\nu}$  and the quantum correction from the functional measure. The interior geometry for  $r < R_s$  is therefore assumed to be described by the MGD metric

$$ds^2 = -e^{\nu^-(r)} dt^2 + \left[1 - \frac{2\hat{m}(r)}{r}\right]^{-1} dr^2 + r^2 d\Omega^2, \quad (46)$$

where the interior mass function is given by

$$\hat{m}(r) = m(r) - \frac{r}{2} \alpha f^-(r), \quad (47)$$

with  $m$  defined in Eq. (37) and  $f^- = f^\diamond$  is the MGD introduced in Eq. (39) for  $r < R_s$ .

The metric (46) must match the outer geometry at  $r = R_s$ , which we write as

$$ds^2 = -e^{\nu^+(r)} dt^2 + e^{\lambda^+(r)} dr^2 + r^2 d\Omega^2, \quad (48)$$

where  $\nu^+(r)$  and  $\lambda^+(r)$  are determined by the field equations (24) for  $r > R_s$ . In particular,  $T_{\mu\nu}^{(M)} = 0$  and we also assumed the imaginary quantum correction is negligible outside compact sources, which only leaves a possible contribution from  $\theta_{\mu\nu}$  for  $r > R_s$ . The outer geometry will therefore be given by a MGD of the Schwarzschild metric,

$$ds^2 = -\left(1 - \frac{2\mathcal{M}}{r}\right) dt^2 + \left(1 - \frac{2\mathcal{M}}{r} + \alpha f^+\right)^{-1} dr^2 + d\Omega^2, \quad (49)$$

where  $\mathcal{M}$  is the Arnowitt-Deser-Misner (ADM) mass of the system and the MGD  $f^+ = f^\diamond(r)$  is determined by the field Eqs. (42a)-(42c) for  $r > R_s$ .

Continuity of the metric across the star surface implies

$$\nu^-(R_s) = \nu^+(R_s) = 1 - \frac{2\mathcal{M}}{R_s}, \quad (50)$$

and

$$1 - \frac{2M_0}{R_s} + \alpha f_s^- = 1 - \frac{2\mathcal{M}}{R_s} + \alpha f_s^+, \quad (51)$$

where  $M_0 = m(R_s)$  and we defined  $F_s^\pm \equiv \lim_{r \rightarrow \pm R_s} F(r)$  for any function  $F$ .

Continuity of the extrinsic curvature of the surface  $r = R_s$  along with the field Eq. (24) imply

$$p_s + \alpha (\theta_1^1)_s^- - i\bar{\zeta}\rho = \alpha (\theta_1^1)_s^+, \quad (52)$$

where  $\rho_s \equiv \rho^-(R_s)$  and  $p_s \equiv p^-(R_s)$ , since  $\rho = p = 0$  for  $r > R_s$ . Using Eq. (42b) for the inner and outer geometries to eliminate  $\theta_1^1$  then implies

$$\kappa p_s + \frac{\alpha f_s^-}{R_s(R_s - 2\mathcal{M})} - i\kappa \bar{\zeta}\rho = \frac{\alpha f_s^+}{R_s(R_s - 2\mathcal{M})}. \quad (53)$$

We note that the limit  $\alpha = \zeta = 0$  reproduces the standard condition  $p_s = 0$  for matching the isotropic fluid interior with an exact Schwarzschild metric in the exterior. If the outer geometry is still given by the Schwarzschild metric with additional sources and quantum corrections,  $f^+ = 0$  and one might have a solid crust with  $p_s < 0$  [102]. In this case, the imaginary quantum correction might induce an instability, although we notice that this contribution vanishes at the surface if the density  $\rho_s = 0$ .

#### IV. MINIMAL GEOMETRIC DEFORMATION OF TOLMAN IV STARS WITH QUANTUM GRAVITY CORRECTIONS

We can now apply the general formalism of Section III to a particular solution of GR representing a compact object. Following Refs. [4, 103], we shall consider the Tolman IV star of total mass  $M_0$  and radius  $R_s$  satisfying the Buchdahl constraint for the compactness  $M_0/R_s < 4/9$ , whose density and isotropic pressure are given by

$$\kappa \rho = \frac{3A^4 M_0 + A^2(3R_s^3 + 7M_0 r^2) + 2r^2(R_s^3 + 3M_0 r^2)}{R_s^3(A^2 + 2r^2)^2} \quad (54a)$$

$$\kappa p = \frac{R_s^3 - M_0(A^2 + 3r^2)}{R_s^3(A^2 + 2r^2)}. \quad (54b)$$

The corresponding interior metric, for  $r < R_s$ , is of the form in Eq. (36) with

$$e^{\xi^-} = \left(1 - \frac{3M_0}{R_s}\right) \left(1 + \frac{r^2}{A^2}\right) = e^{\nu^-} \quad (55a)$$

$$\mu^- = \frac{A^2}{A^2 + 2r^2} \left(1 - \frac{M_0 r^2}{R_s^3}\right) \left(1 + \frac{r^2}{A^2}\right). \quad (55b)$$

The constant  $A$  can be expressed in terms of the unperturbed ADM mass  $M_0$  by matching continuously the interior metric with the outer Schwarzschild geometry across  $r = R_s$ , which yields

$$A^2 = \frac{R_s^3}{M_0} \left(1 - \frac{3M_0}{R_s}\right). \quad (56)$$

One then finds the metric functions

$$e^{\nu^-} = 1 - (3 - x^2)X \quad (57a)$$

$$\mu^- = \frac{1 - X[3 - x^2(3 - x^2)X]}{1 - (3 - 2x^2)X}, \quad (57b)$$

where we introduced the compactness  $X \equiv M_0/R_s$  and the dimensionless radial coordinate  $x = r/R_s$  for convenience. Likewise, we have

$$\kappa R_s^2 \rho = 3X \frac{2 + X [2x^4 X + x^2(3 - 7X) - 9(1 - X)]}{[1 - (3 - 2x^2)X]^2}, \quad (58a)$$

$$\kappa R_s^2 p = \frac{3(1-x^2)X^2}{1 - (3 - 2x^2)X}. \quad (58b)$$

We remark that, according to the procedure described in Section III, the metric functions  $\nu$  in Eq. (57a) and  $\mu$  in Eq. (57b) represent the seed metric for the MGD satisfying Eqs. (40a)-(40c) in which the density  $\rho$  and isotropic pressure  $p$  are given in Eqs. (58a) and (58b).

We next consider an MGD of the above solution which preserves the outer Schwarzschild geometry (49) with  $\mathcal{M} = M_0$  and  $f^+ = 0$ . The matching Eq. (52), can be solved by imposing the so-called mimic constraint, now modified by the quantum correction, that is

$$\theta_1^1 = p + i\bar{\zeta}\rho. \quad (59)$$

Following Eq. (40b), the above can be expressed as <sup>4</sup>

$$\kappa \alpha R_s^2 \theta_1^1 = \frac{1}{x^2} + \mu \left( \frac{1}{x^2} + \frac{\dot{\nu}}{x} \right), \quad (60)$$

where the dots represent derivatives with respect to  $x$ , that is  $\dot{F} = R_s F'$  for any function  $F$ . The interior MGD follows from Eq. (42b) and reads

$$\alpha f^- = \mu^- + \frac{1}{1 + x\dot{\nu}^-} \left[ 1 - 2i\bar{\zeta}x^2 R_s^2 \left( 1 - \frac{1}{\alpha} \right) \rho \right], \quad (61)$$

implying that the interior metric encodes corrections due to quantum gravity and the deformed metric element is given by

$$e^{-\lambda^-} = 2\mu + R_s^2 \left( \frac{1 - 3X + x^2 X}{1 - 3X + 3x^2 X} \right) + 8i\bar{\zeta}x^2 R_s^2 \left\{ 1 + (1 - 6X)^2 \frac{Xx^2}{1 - 3X} \log \left[ (1 - 3X)^2 \left( 1 + \frac{Xx^2}{1 - 3X} \right) \right] \right\} \left( 1 - \frac{1}{\alpha} \right) \rho, \quad (62)$$

where again Eq. (39) was employed additionally to Eq. (57a). We now need to deal with the imaginary part of the metric function (62). As we mentioned in the Introduction, a straightforward option which preserves the time independence is given by taking the modulus of Eq. (62). Since we are mainly interested in the effects induced by the quantum measure, we Taylor-expand it in the

<sup>4</sup> We shall omit the superscripts  $\pm$  for simplicity when there is no confusion.

running parameter  $\bar{\zeta} \sim \zeta$  and just keep the leading order, that is

$$e^{-\lambda^-} \simeq 2\mu + R_s^2 \left( \frac{1 - 3X + x^2 X}{1 - 3X + 3x^2 X} \right) + 4 \frac{\bar{\zeta}^2}{\alpha^2} x^4 R_s^4 \frac{\left\{ 1 + (1 - 6X)^2 \frac{X x^2}{1 - 3X} \log \left[ (1 - 3X)^2 \left( 1 + \frac{X x^2}{1 - 3X} \right) \right] \right\}^2}{2\mu + R_s^2 \left( \frac{1 - 3X + x^2 X}{1 - 3X + 3x^2 X} \right)} (\alpha - 1)^2 \rho^2, \quad (63)$$

It is worth mentioning that the limit  $\alpha \rightarrow 1$  suppresses all quantum corrections to the metric term, as the imaginary term in the metric component (63) vanishes. Also, if the MGD parameter  $\alpha$  tends to zero, the quantum measure parameter  $\bar{\zeta}$  must go to zero faster, to avoid divergences in the imaginary term.

It is instructive to write the metric component (63) in polar form as  $e^{-\lambda^-} = \Theta e^{i\Phi}$ , where

$$\Theta = \left\{ 32 \frac{\bar{\zeta}^2}{\alpha^2} R_s^4 x^4 (\alpha - 1)^2 \rho^2 \left( 1 + \frac{X(x - 6xX)^2}{1 - 3X} \log \left[ (1 - 3X)^2 ((x^2 - 3)X + 1) \right] \right)^2 + \left[ \frac{R^2 ((x^2 - 3)X + 1)}{3(x^2 - 1)X + 1} - \frac{X((x^2 - 3)x^2 X + 3) - 1}{(2x^2 - 3)X + 1} \right]^2 \right\}^{1/2} \quad (64)$$

and <sup>5</sup>

$$\Phi = \arctan \left[ -\frac{8\bar{\zeta} R_s^2 x^2}{\alpha k(x, X)} \rho(x) (3(x^2 - 1)X + 1) ((2x^2 - 3)X + 1) (\alpha - 1)^2 (x^2 X (1 - 6X))^2 \times \log \left( (1 - 3X)^2 ((x^2 - 3)X + 1) - 3X + 1 \right) \right]. \quad (65)$$

Since only the metric component (A9) is complex and  $-\pi/2 \leq \arctan(b) \leq \pi/2$ , for any argument  $b \in \mathbb{R}$  (in particular the one in Eq. (A12)), the MGD metric component satisfies the criterion dictated by the KS theorem [70].

The MGD metric components can now be matched with the outer Schwarzschild solution (49) with  $f^+ = 0$ . Continuity expressed by Eqs. (50) and (51) leads to the ADM mass

$$\mathcal{M} \simeq M_0 + \frac{R_s}{2} (1 - 4X) + \frac{8\bar{\zeta}^2 (\alpha - 1)^2 R_s^5}{\alpha^2 (1 - X)^2} \left\{ 1 + \frac{X(1 - 6X)^2}{1 - 3X} \log \left[ (1 - 3X)(1 - 2X) \right] \right\}^2 \rho^2, \quad (66)$$

where Eq. (37) was used. The quantum gravity correction proportional to  $\bar{\zeta}^2$  becomes comparable to the MGD for  $|\bar{\zeta}| \simeq |\alpha|$ . Eq. (59) implies that the magnitude of the effective radial pressure in Eq. (33) reads

$$\dot{p}_r = \frac{3X^2(1 - x^2)}{\kappa R_s^2 (1 - 3X + 2x^2 X)} + \frac{\bar{\zeta}^2 v(x) X^2 (\alpha - 1)^2}{\alpha^2 \kappa (x^2 X - 1)^4} \left[ x^2 X (2(x^2 - 3)X + 3) + 9X(X - 1) + 2 \right]^2, \quad (67)$$

<sup>5</sup> The explicit form of  $k = k(x, X)$  is not relevant for the following argument.



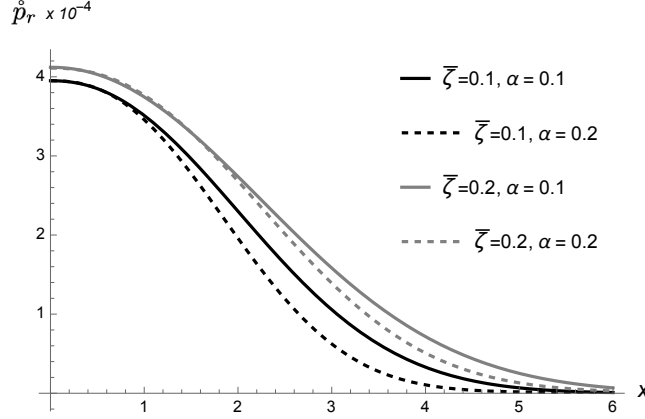


FIG. 1: Effective radial pressure  $\hat{p}_r$  of a stellar distribution of compactness  $X = 0.25$ , as a function of the radial coordinate, for different values of  $\bar{\zeta}$  and  $\alpha$ .

where

$$v(x) \equiv \frac{(1 - 3X - 2Xx^2)(1 - x^2)}{\kappa(1 - 3X + 4Xx^2)^2} \left[ 1 + (1 - 6X)^2 \frac{Xx^2}{1 - 3X} \log \left[ (1 - 3X)^2 \left( 1 + \frac{Xx^2}{1 - 3X} \right) \right] \right]^2. \quad (68)$$

It is worth mentioning that quantum gravity effects can be read off in the effective radial pressure (67) in the term accompanying the running parameter  $\bar{\zeta}$ .

The effective radial pressure (67) is displayed in Fig. 1 as a function of the radial coordinate, for different values of the parameter  $\bar{\zeta}$  governing quantum gravity corrections and also for two non-trivial values of the GD charge  $\alpha$ . Quantum gravity effects implemented by the parameter  $\bar{\zeta}$  in Eq. (67) show that the effective central radial pressure when  $\bar{\zeta} = 0.2$  is 4.3% higher, when compared to  $\bar{\zeta} = 0.1$ , for fixed values of the GD hairy charge. For fixed values of  $\bar{\zeta}$ , the higher the GD hairy charge  $\alpha$ , the steepest the decrement of the effective radial pressure is. It indicates that GD effects attenuate the effective radial pressure profile along the radial coordinate.

The effective density reads

$$\begin{aligned} \hat{\rho} = & \frac{X [2X^3 x^2 (3Xx^2 + 1) + (1 - 3X)^2 X (7Xx^2 + 3) + 3(1 - 3X)^4 R_s^4]}{\kappa [2X^2 x^2 + (1 - 3X)^2 R_s^2]^2} \\ & + \frac{6\alpha X [X(x^2 - 3) + 1]}{R_s^2 [3X(x^2 - 1) + 1]^2} + i \left( 1 - \frac{1}{\alpha} \right) \bar{\zeta} w(x) \frac{X^2 v(x)(x^2 - 1)}{(4Xx^2 - 3X + 1)^2}, \end{aligned} \quad (69)$$

where

$$w = \frac{9(2x^4 - 3x^2 + 2)}{16\kappa^2 (x^2 - 1)^5 R_s^4} [x^6(4X - 2) + x^4(19 - 24X) + x^2(38X - 33) - 22X + 20]. \quad (70)$$

As already mentioned, the imaginary part of the effective energy density in Eq. (69) corresponds to the instability of the degrees of freedom in the hydrodynamical fluid, measuring the fluid lifetime.

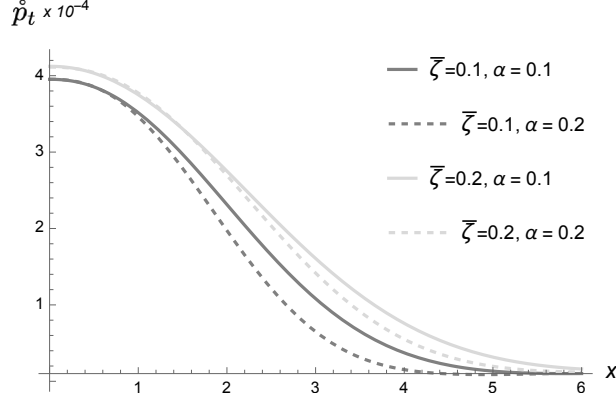


FIG. 2: Effective tangential pressure  $\hat{p}_t$  of a stellar distribution of compactness  $X = 0.25$ , as a function of the radial coordinate, for different values of  $\bar{\zeta}$  and  $\alpha$ .

This interpretation holds, in particular, for the case of the quark-gluon plasma, which is expected to play a decisive role in the core of neutron and quark stars [86].

The effective tangential pressure, after Taylor-expanding it in terms of the quantum gravity parameter  $\zeta$  up to fourth order, reads

$$\begin{aligned} \hat{p}_t \simeq & \frac{3X^4(1-x^2)}{\kappa R_s^2(1-3X+2x^2X)} + \frac{Xx^2}{\kappa(x^2-1)+1} \\ & + \frac{2\bar{\zeta}^2}{\alpha^2} w(x) \frac{X\kappa v^2(x)R_s^2(x^2-1)(\alpha-1)^2}{3(4Xx^2-3X+1)^2} (2Xx^2-1+3X). \end{aligned} \quad (71)$$

Fig. 2 shows this effective tangential pressure as a function of the radial coordinate, for several values of the parameter  $\bar{\zeta}$ . The anisotropic factor is illustrated in Figs. 3 and 4 as a function of the radial coordinate, for different values of  $\bar{\zeta}$  and  $\alpha$ . Those graphs show that the anisotropy increases towards the stellar surface.

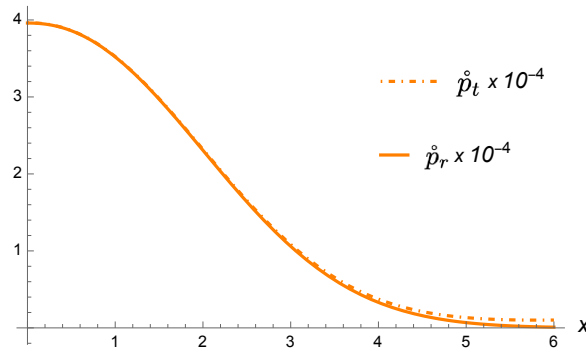


FIG. 3: Effective tangential and radial pressures of a stellar distribution of compactness  $X = 0.25$ , as a function of the radial coordinate, for  $\bar{\zeta} = 0.1$  and  $\alpha = 0.1$ .

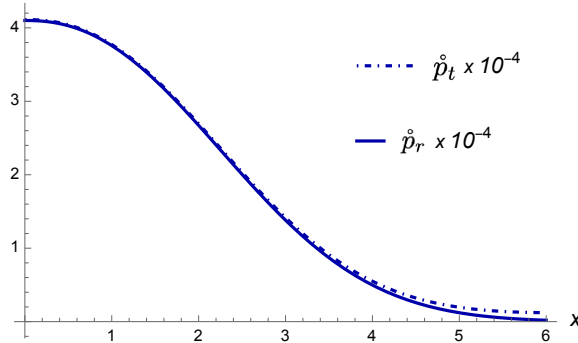


FIG. 4: Effective tangential and radial pressures of a stellar distribution of compactness  $X = 0.25$ , as a function of the radial coordinate, for  $\bar{\zeta} = 0.2$  and  $\alpha = 0.2$ .

An interesting quantity to consider is the surface redshift, which depends on both  $\bar{\zeta}$  and  $\alpha$  and can be expressed as

$$z(\alpha, \zeta) = \frac{1}{\sqrt{1 - \frac{2\mathcal{M}(\alpha, \bar{\zeta})}{R_s}}} - 1. \quad (72)$$

It can be directly obtained from the ADM mass in Eq. (66) and is displayed in Fig. 5, as a function of the MGD charge  $\alpha$  and the quantum gravity parameter  $\zeta$ . The anisotropic factor amplifies the gravitational redshift at the stellar surface. Therefore, for each fixed value of  $\zeta$ , a distant observer detects a more compact stellar distribution for  $\alpha > 0$ , when compared to the isotropic case. Reciprocally, for each fixed value of the GD charge  $\alpha$ , a distant observer sees a stellar distribution that is more compact, for  $\bar{\zeta} > 0$ . When  $\bar{\zeta} \rightarrow 0$  the redshift is a function of the hairy charge  $\alpha$  only and reproduces the result in Ref. [4]. The larger the magnitude of quantum gravity effects driven by  $\bar{\zeta}$ , the bigger the surface redshift. These features comply with Eq. (66), which in particular states that  $\mathcal{M} > M_0$ . They are also compatible with the recent bounds for the surface redshift in realistic anisotropic stellar models.

The upper limit  $z = 5.211$  was obtained for compact stellar distributions that satisfy dominant energy conditions (DEC) in Ref. [104]. It yields the upper bounds  $\bar{\zeta}_{\max} = 2.18$ , when  $\alpha = 0.4$ , and  $\bar{\zeta}_{\max} = 2.268$ , for  $\alpha = 0.2$ . The upper limit  $z = 3.840$ , for strong energy conditions (SEC) yield, apiece, the upper bounds  $\bar{\zeta}_{\max} = 2.088$ , when  $\alpha = 0.4$ , and  $\zeta_{\max} = 2.009$ , for  $\alpha = 0.2$ . More generally, the upper bounds  $\zeta_{\max}$ , with  $\alpha$  varying, are plotted in Fig. 6. Higher values of  $\alpha$  lower the maximum value  $\bar{\zeta}_{\max}$ . We remark the fact that  $\alpha$  and  $\bar{\zeta}$  are completely independent, as they respectively represent the MGD and the functional measure as different sources. Fig. 6 illustrates the fact that the upper bound on the redshift implies an upper bound  $\bar{\zeta}_{\max}$  on the parameter  $\bar{\zeta}$ , for each fixed value in the range  $10^{-5} \leq \alpha \leq 0.4$  considered. Higher magnitudes of the GD hairy

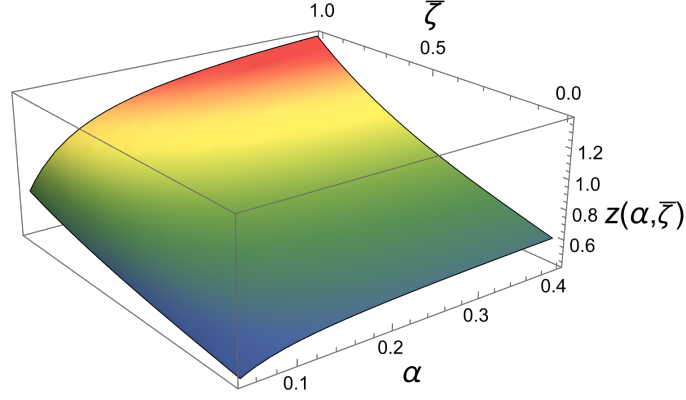


FIG. 5: Anisotropic surface redshift of a stellar distribution of compactness  $X = 0.25$ , as a function of the GD hairy parameter  $\alpha$  and the quantum gravity parameter  $\bar{\zeta}$ .

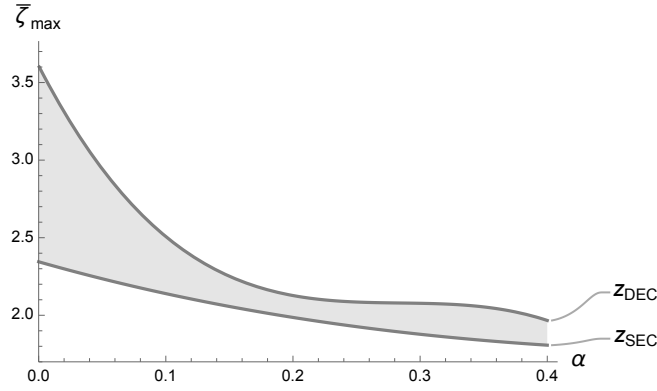


FIG. 6: Upper bounds  $\bar{\zeta}_{\max}$  as a function of  $\alpha$ , for  $10^{-5} \leq \alpha \leq 0.4$ , according to the bounds  $z_{\text{SEC}} = 3.840$  and  $z_{\text{DEC}} = 5.211$  on the surface redshift [104].

charge  $\alpha$  induce suppression of  $\bar{\zeta}_{\max}$ . The numerical results can be interpolated by the polynomial curve,

$$\bar{\zeta}_{\max}^{\text{DEC}} \simeq -65.077\alpha^3 + 55.544\alpha^2 - 15.907\alpha + 3.7076, \quad (73)$$

for the upper bound  $z_{\text{DEC}} = 5.211$  on the surface redshift, and by

$$\bar{\zeta}_{\max}^{\text{SEC}} \simeq -1.1329\alpha^3 + 2.9280\alpha^2 - 2.3338\alpha + 2.3448, \quad (74)$$

for the upper bound  $z_{\text{SEC}} = 3.840$ , both with interpolation errors  $< 10^{-4}$ .

Different choices for the mimic constraints are analysed in Appendix A.

## V. CONCLUSIONS

We have studied the influence of the functional measure in the 1-loop effective action of quantum gravity within the GD approach. The most striking feature induced by the functional measure is the addition of imaginary terms in the effective energy-momentum tensor that sources the Einstein field equations. One generally expects that such terms reflect inherent instabilities.

For a suitable choice of the mimic constraint to preserve the outer Schwarzschild vacuum, we showed that it naturally generates complex metric functions that satisfy the KS criterium, showing the compatibility between the metric solutions obtained and the QFT side of quantum gravity. Effective field equations for compact stellar objects were therefore implemented in the context of both the GD and quantum gravity to generate consistent solutions for the interior of a compact object. The role of both the GD and quantum gravity on the profiles of the effective radial and tangential pressures, as well as on the effective energy density, was analysed for compact self-gravitating anisotropic stellar distributions obtained from the Tolman IV family of solutions.

For a different choice of the mimic constraint detailed in Appendix A 1, the GD method coupled with the additional imaginary term due to the functional measure can still accommodate real metrics, only affecting the hidden sector represented by the GD term in the energy-momentum in the Einstein equations. It is a consequence of the modified mimic constraint and the cancellation of the functional measure contribution in the outer region of the stellar distribution.

Finally, we studied the absolute bounds on the surface redshift of a stellar distribution. Other mimic constraints and extensions considered in Ref. [4] can be also employed in the context of the functional measure. The upper bounds  $\bar{\zeta}_{\max}$  are then higher, showing that the mimic constraint for the pressure provides the most stringent upper limits to the parameter regulating quantum gravity effects.

### *Acknowledgments*

R.C. is partially supported by the INFN grant FLAG and his work has also been carried out in the framework of activities of the National Group of Mathematical Physics (GNFM, INdAM). I.K. thanks the National Council for Scientific and Technological Development – CNPq (Grant No. 303283/2022-0) for financial support. R.d.R. thanks to The São Paulo Research Foundation – FAPESP (Grants No. 2021/01089-1 and No. 2022/01734-7), CNPq (Grants No. 303742/2023-2 and No. 401567/2023-0), and the Coordination for the Improvement of Higher Education Personnel

(CAPES-PrInt 88887.897177/2023-00), for partial financial support. R.dR. thanks R.C. and DIFA, Università di Bologna, for the hospitality.

### Appendix A: Alternative mimic constraints

We provide here details about different implementations of the mimic constraint that preserve the outer Schwarzschild metric.

#### 1. Case I

We note that the matching condition in Eq. (52) can also be solved by imposing

$$\alpha \theta_1^1 = p + i \bar{\zeta} \rho , \quad (\text{A1})$$

which, according to Eq. (40b), can be written as

$$\kappa \alpha R_s^2 \theta_1^1 = \frac{1}{x^2} + \mu \left( \frac{1}{x^2} + \frac{\dot{\nu}}{x} \right) + i \kappa R_s^2 \bar{\zeta} \rho , \quad (\text{A2})$$

The interior MGD deformation is then determined by Eq. (42b). The imaginary contribution due to the functional measure drops out and the metric remains real, as

$$\alpha f^- = \mu^- + \frac{1}{1 + x \dot{\nu}^-} , \quad (\text{A3})$$

which yields

$$e^{-\lambda^-} = \mu^- + \alpha f^- = 2 \mu^- + \frac{1}{1 + x \dot{\nu}^-} . \quad (\text{A4})$$

Continuity expressed by Eqs. (50) and (51) leads to the ADM mass

$$\mathcal{M} = \frac{R_s}{2} = M_0. \quad (\text{A5})$$

This case is therefore rather trivial and no modifications from both the GD hairy charge and the parameter encoding quantum gravity effects are obtained.

#### 2. Case II

Let us finally consider

$$\alpha \theta_1^1 = p , \quad (\text{A6})$$

which, following Eq. (40b), can be expressed as

$$\kappa \alpha R_s^2 \theta_1^1 = \frac{1}{x^2} + \mu \left( \frac{1}{x^2} + \frac{\dot{\nu}}{x} \right). \quad (\text{A7})$$

The interior MGD comes from Eq. (42b), that is

$$\alpha f^- = \mu^- + \frac{1}{1+x\dot{\nu}^-} (1 - 2i\bar{\zeta} x^2 R_s^2 \rho), \quad (\text{A8})$$

so that

$$\begin{aligned} e^{-\lambda^-} &= 2\mu + R_s^2 \left( \frac{1 - 3X + x^2 X}{1 - 3X + 3x^2 X} \right) \\ &\quad + 8i\bar{\zeta} x^2 R_s^2 \left\{ 1 + (1-6X)^2 \frac{X x^2}{1-3X} \log \left[ (1-3X)^2 \left( 1 + \frac{X x^2}{1-3X} \right) \right] \right\} \rho, \end{aligned} \quad (\text{A9})$$

where again Eq. (39) and (57a) were employed.

We again deal with the imaginary part of the metric function (A9) by taking its modulus. By Taylor-expanding in the running parameter  $\zeta$  and keeping the leading order, we obtain

$$\begin{aligned} e^{-\lambda^-} &\simeq 2\mu + R_s^2 \left( \frac{1 - 3X + x^2 X}{1 - 3X + 3x^2 X} \right) \\ &\quad + 4\bar{\zeta}^2 x^4 R_s^4 \frac{\left\{ 1 + (1-6X)^2 \frac{X x^2}{1-3X} \log \left[ (1-3X)^2 \left( 1 + \frac{X x^2}{1-3X} \right) \right] \right\}^2}{2\mu + R_s^2 \left( \frac{1-3X+x^2 X}{1-3X+3x^2 X} \right)} \rho^2, \end{aligned} \quad (\text{A10})$$

The polar form  $e^{-\lambda^-} = \Theta e^{i\Phi}$  is now given by

$$\begin{aligned} \Theta &= \left\{ 32\bar{\zeta}^2 R_s^4 x^4 \rho^2 \left( 1 + \frac{X(x-6xX)^2}{1-3X} \log \left[ (1-3X)^2 ((x^2-3)X+1) \right] \right)^2 \right. \\ &\quad \left. + \left[ \frac{R^2 ((x^2-3)X+1)}{3(x^2-1)X+1} - \frac{X((x^2-3)x^2X+3)-1}{(2x^2-3)X+1} \right]^2 \right\}^{1/2} \end{aligned} \quad (\text{A11})$$

and

$$\begin{aligned} \Phi &= \arctan \left[ -\frac{8\bar{\zeta} R_s^2 x^2}{k(x, X)} \rho(x) (3(x^2-1)X+1) ((2x^2-3)X+1) (x^2 X(1-6X))^2 \right. \\ &\quad \left. \times \log \left[ (1-3X)^2 ((x^2-3)X+1) - 3X+1 \right] \right], \end{aligned} \quad (\text{A12})$$

where

$$k(x, X) = (3X-1) [(x^2-3)X+1] [(2x^2-3)X-3x^2(x^2-1)X^2+1]. \quad (\text{A13})$$

The MGD metric still satisfies the criterion established in the KS theorem [70].

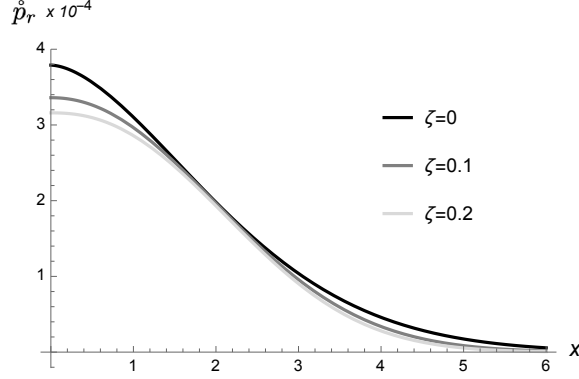


FIG. 7: Effective radial pressure  $\dot{p}_r$  of a stellar distribution of compactness  $X = 0.25$ , as a function of the radial coordinate, for different values of  $\bar{\zeta}$ .

The ADM mass  $\mathcal{M}$  can be expressed as

$$\mathcal{M} \simeq M_0 + \frac{R_s}{2} (1-4X) + \frac{8\bar{\zeta}^2 R_s^5}{(1-X)^2} \left\{ 1 + \frac{X(1-6X)^2}{1-3X} \log[(1-3X)(1-2X)] \right\}^2 \rho^2, \quad (\text{A14})$$

where Eq. (37) was used.

Eq. (A1) implies that the magnitude of the effective radial pressure  $\dot{p}_r = \dot{p}_r(x, \zeta)$  in Eq. (33) reads

$$\dot{p}_r = \frac{3X^2(1-x^2)}{\kappa R_s^2(1-3X+2x^2X)} + \bar{\zeta}^2 v(x) X^2 \frac{[x^2X(2(x^2-3)X+3) + 9X(X-1) + 2]^2}{\kappa(x^2X-1)^4}. \quad (\text{A15})$$

The effective radial pressure (A15) is depicted in Fig. 7 as a function of the radial coordinate, for different values of the parameter  $\zeta$  governing quantum gravity corrections. Quantum gravity effects implemented by the parameter  $\bar{\zeta}$  in Eq. (A15) show that the effective central radial pressure when  $\bar{\zeta} = 0.1$  is 11.3% smaller than when  $\bar{\zeta} = 0$ , whereas for  $\zeta = 0.2$ , this deviation increases up to 19.9%. Although quantum gravity effects make the central radial pressure decrease, for  $x \gtrsim 6$  these values equalize. Fig. 7 also shows that in the range  $1.8 \lesssim x \lesssim 2.4$  the values of the effective radial pressure are essentially the same.

The effective tangential pressure, after Taylor-expanding it in terms of the quantum gravity parameter  $\bar{\zeta}$  up to  $\mathcal{O}(\bar{\zeta}^4)$ , reads

$$\begin{aligned} \dot{p}_t(x, \bar{\zeta}) = & \frac{3X^4(1-x^2)}{\kappa R_s^2[1-3X+2x^2X]} + \frac{Xx^2}{\kappa(x^2-1)+1} \\ & + 2\bar{\zeta}^2 w(x) \frac{X\kappa v^2(x)R_s^2(x^2-1)[(2Xx^2-1+3X)]}{3(4Xx^2-3X+1)^2}. \end{aligned} \quad (\text{A16})$$

Fig. 8 shows the effective tangential pressure  $\dot{p}_t$  profile (A16) as a function of the radial coordinate, for several values of the parameter  $\zeta$ . Quantum gravity effects induce the central tangential pressure



also to decrease, although at a lower rate, compared to the effective radial pressure. For  $r \gtrsim 6.0$  these values also equalize. Fig. 8 shows that in the range  $1.9 \lesssim x \lesssim 2.3$  the values of the effective tangential pressure attain very similar values.

The anisotropic factor is illustrated in Figs. 9-11 as a function of the radial coordinate, for different values of  $\bar{\zeta}$ , as the difference between the effective tangential and radial pressures of a stellar distribution of compactness  $X = 0.25$ , for different values of  $\bar{\zeta}$ . One can see that the anisotropy factor increases towards the stellar surface. The effective tangential pressure decreases as a function of the radial coordinate, however at a lower rate, compared to the effective radial pressure. For  $x \gtrsim 2.0$  the difference between the effective radial and the tangential pressures is already noticeable and attains a maximum value at  $x \sim 6.0$ .

The surface redshift (72) is displayed in Fig. 12, as a function of the quantum gravity parameter  $\bar{\zeta}$ . Anisotropy is shown to amplify the gravitational redshift at the stellar surface. Therefore, for each fixed value of  $\bar{\zeta}$ , a distant observer detects a more compact stellar distribution, when compared to the isotropic case corresponding to  $\bar{\zeta} \rightarrow 0$ , where no quantum gravity effects set in. The larger the magnitude of quantum gravity effects driven by  $\bar{\zeta}$ , the bigger the surface redshift is. These features comply with Eq. (A14), which in particular states that  $\mathcal{M} > M_0$ . They are also compatible with the recent bounds for the surface redshift in realistic anisotropic stellar models.

The upper limit  $z = 5.211$  was obtained for the redshift of compact stellar distributions that satisfy dominant energy conditions (DEC) in Ref. [104] and yield, the upper bound  $\zeta_{\max} = 2.373$ . The redshift upper limit  $z = 3.840$ , for strong energy conditions (SEC) yields the upper bound  $\bar{\zeta}_{\max} = 2.072$ .

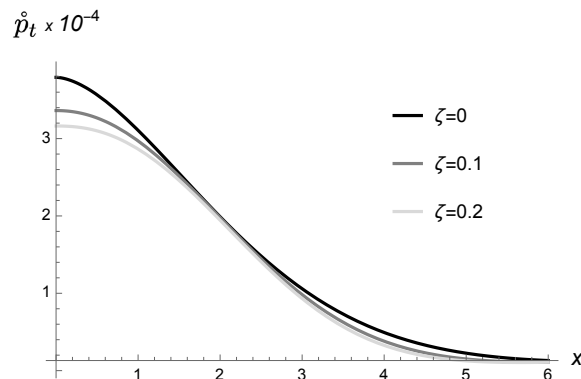


FIG. 8: Effective tangential pressure  $\mathring{p}_t$  of a stellar distribution of compactness  $X = 0.25$ , as a function of the radial coordinate, for different values of  $\zeta$ .

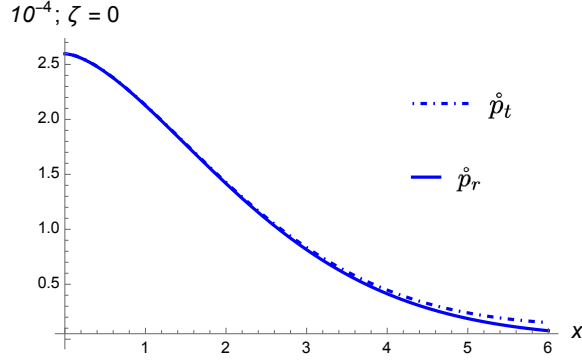


FIG. 9: Effective tangential and radial pressures of a stellar distribution of compactness  $X = 0.25$ , as a function of the radial coordinate, for  $\bar{\zeta} = 0$ .

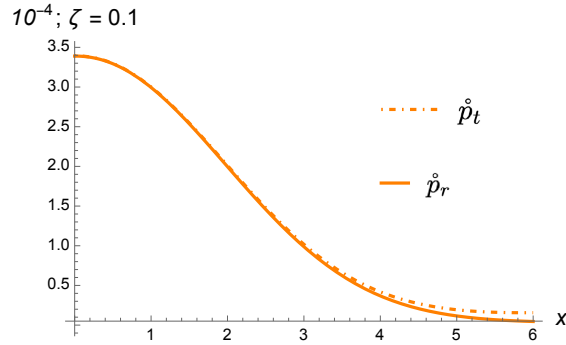


FIG. 10: Effective tangential and radial pressures of a stellar distribution of compactness  $X = 0.25$ , as a function of the radial coordinate, for  $\bar{\zeta} = 0.1$ .

- 
- [1] Abbott B P *et al.* (LIGO Scientific, Virgo) 2016 *Phys. Rev. Lett.* **116** 221101 [Erratum: *Phys.Rev.Lett.* 121, 129902 (2018)] (*Preprint* 1602.03841)
  - [2] Ovalle J 2017 *Phys. Rev.* **D95** 104019 (*Preprint* 1704.05899)
  - [3] Ovalle J 2019 *Phys. Lett.* **B788** 213–218 (*Preprint* 1812.03000)
  - [4] Ovalle J, Casadio R, da Rocha R and Sotomayor A 2018 *Eur. Phys. J.* **C78** 122 (*Preprint* 1708.00407)
  - [5] Ovalle J 2008 *Mod. Phys. Lett.* **A23** 3247 (*Preprint* gr-qc/0703095)
  - [6] Ovalle J, Casadio R, da Rocha R, Sotomayor A and Stuchlik Z 2018 *EPL* **124** 20004 (*Preprint* 1811.08559)
  - [7] Antoniadis I, Arkani-Hamed N, Dimopoulos S and Dvali G R 1998 *Phys. Lett.* **B436** 257 (*Preprint* 9804398)
  - [8] da Rocha R and Hoff da Silva J M 2012 *Phys. Rev. D* **85** 046009 (*Preprint* 1202.1256)
  - [9] Abdalla M C B, Hoff da Silva J M and da Rocha R 2009 *Phys. Rev.* **D80** 046003 (*Preprint* 0907.1321)
  - [10] Ferreira-Martins A J and da Rocha R 2021 *Nucl. Phys. B* **973** 115603 (*Preprint* 2104.02833)

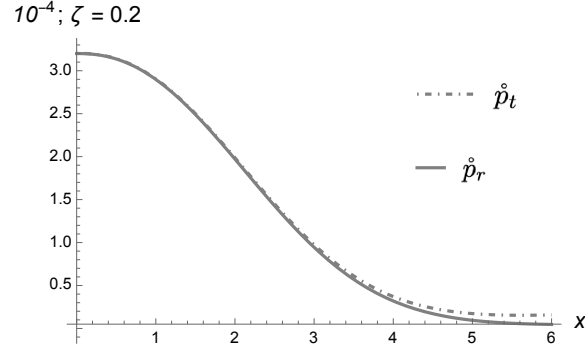


FIG. 11: Effective tangential and radial pressures of a stellar distribution of compactness  $X = 0.25$ , as a function of the radial coordinate, for  $\bar{\zeta} = 0.2$ .

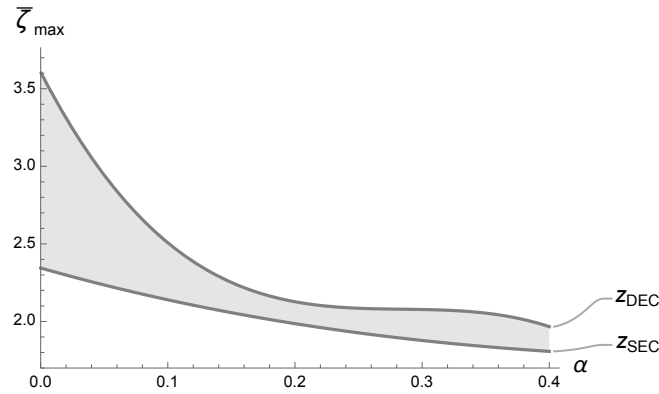


FIG. 12: Anisotropic surface redshift of a stellar distribution of compactness  $X = 0.25$ , as a function of the quantum gravity parameter  $\bar{\zeta}$ .

- [11] Sharif M and Naseer T 2023 *Chin. J. Phys.* **86** 596–615
- [12] Estrada M 2019 *Eur. Phys. J.* **C79** 918 (*Preprint* 1905.12129)
- [13] Gabbanelli L, Ovalle J, Sotomayor A, Stuchlik Z and Casadio R 2019 *Eur. Phys. J.* **C79** 486 (*Preprint* 1905.10162)
- [14] Leon P and Las Heras C 2023 *Eur. Phys. J. C* **83** 260
- [15] Avalos R, Bargeño P and Contreras E 2023 *Fortsch. Phys.* **2023** 2200171 (*Preprint* 2303.04119)
- [16] Contreras E and Stuchlik Z 2022 *Eur. Phys. J. C* **82** 706 (*Preprint* 2208.09028)
- [17] Maurya S K, Singh K N and Nag R 2021 *Chin. J. Phys.* **74** 1539
- [18] Singh K N, Maurya S K, Dutta A, Rahaman F and Aktar S 2021 *Eur. Phys. J. C* **81** 909 (*Preprint* 2110.03182)
- [19] Maurya S K, Tello-Ortiz F and Govender M 2021 *Fortsch. Phys.* **69** 2100099
- [20] Maurya S K, Errehymy A, Jasim M K, Daoud M, Al-Harbi N and Abdel-Aty A H 2023 *Eur. Phys. J. C* **83** 317
- [21] Singh K N, Banerjee A, Maurya S K, Rahaman F and Pradhan A 2021 *Phys. Dark Univ.* **31** 100774

- (Preprint 2007.00455)
- [22] Ramos A, Arias C, Fuenmayor E and Contreras E 2021 *Eur. Phys. J. C* **81** 203 (Preprint 2103.05039)
- [23] Casadio R, Contreras E, Ovalle J, Sotomayor A and Stuchlick Z 2019 *Eur. Phys. J.* **C79** 826 (Preprint 1909.01902)
- [24] Sharif M and Naseer T 2023 *Phys. Dark Univ.* **42** 101324 (Preprint 2310.00872)
- [25] Rincón A, Gabbanelli L, Contreras E and Tello-Ortiz F 2019 *Eur. Phys. J.* **C79** 873 (Preprint 1909.00500)
- [26] Tello-Ortiz F, Maurya S K, Errehymy A, Singh K and Daoud M 2019 *Eur. Phys. J.* **C79** 885
- [27] Morales E and Tello-Ortiz F 2018 *Eur. Phys. J.* **C78** 841 (Preprint 1808.01699)
- [28] Panotopoulos G and Rincón A 2018 *Eur. Phys. J.* **C78** 851 (Preprint 1810.08830)
- [29] Singh K, Maurya S K, Jasim M K and Rahaman F 2019 *Eur. Phys. J.* **C79** 851
- [30] Jasim M K, Maurya S K, Khalid Jassim A, Mustafa G, Nag R and Saif Al Buwaiqi I 2023 *Phys. Scripta* **98** 045305
- [31] Gabbanelli L, Rincón A and Rubio C 2018 *Eur. Phys. J.* **C78** 370 (Preprint 1802.08000)
- [32] Pérez Graterol R 2018 *Eur. Phys. J. Plus* **133** 244
- [33] Heras C L and Leon P 2018 *Fortsch. Phys.* **66** 1800036 (Preprint 1804.06874)
- [34] Torres-Sánchez V A and Contreras E 2019 *Eur. Phys. J.* **C79** 829 (Preprint 1908.08194)
- [35] Hensh S and Stuchlík Z 2019 *Eur. Phys. J.* **C79** 834
- [36] Contreras E, Rincón A and Bargeño P 2019 *Eur. Phys. J.* **C79** 216 (Preprint 1902.02033)
- [37] Tello-Ortiz F, Maurya S K and Bargeño P 2021 *Eur. Phys. J. C* **81** 426
- [38] Sharif M and Ama-Tul-Mughani Q 2020 *Annals Phys.* **415** 168122 (Preprint 2004.07925)
- [39] Contreras E and Bargeño P 2019 *Class. Quant. Grav.* **36** 215009 (Preprint 1902.09495)
- [40] Andrade J, Ortega K Y, Klínger W N R, Copa R C G, Medina S S C and Cruz J D 2023 *Eur. Phys. J. C* **83** 1085
- [41] Zubair M, Azmat H and Jameel H 2023 *Eur. Phys. J. C* **83** 905
- [42] Bamba K, Bhatti M Z, Yousaf Z and Shoukat Z 2023 *Eur. Phys. J. C* **83** 1033 (Preprint 2307.10399)
- [43] Maurya S K, Mustafa G, Ray S, Dayanandan B, Aziz A and Errehymy A 2023 *Phys. Dark Univ.* **42** 101284
- [44] Tello-Ortiz F, Bargeño P, Alvarez A and Contreras E 2023 *Fortsch. Phys.* **71** 2200170
- [45] Contreras E and Fuenmayor E 2021 *Phys. Rev. D* **103** 124065 (Preprint 2107.01140)
- [46] Sharif M and Majid A 2020 *Chin. J. Phys.* **68** 406–418
- [47] Maurya S K, Errehymy A, Singh K N, Tello-Ortiz F and Daoud M 2020 *Phys. Dark Univ.* **30** 100640 (Preprint 2003.03720)
- [48] Ovalle J, Casadio R, Contreras E and Sotomayor A 2021 *Phys. Dark Univ.* **31** 100744 (Preprint 2006.06735)
- [49] Ovalle J, Contreras E and Stuchlick Z 2021 *Phys. Rev. D* **103** 084016 (Preprint 2104.06359)
- [50] Contreras E, Ovalle J and Casadio R 2021 *Phys. Rev. D* **103** 044020 (Preprint 2101.08569)

- [51] da Rocha R 2020 *Phys. Rev. D* **102** 024011 (*Preprint* 2003.12852)
- [52] da Rocha R and Tomaz A A 2019 *Eur. Phys. J. C* **79** 1035 (*Preprint* 1905.01548)
- [53] da Rocha R and Tomaz A A 2020 *Eur. Phys. J. C* **80** 857 (*Preprint* 2005.02980)
- [54] Shiromizu T, Maeda K i and Sasaki M 2000 *Phys. Rev.* **D62** 024012 (*Preprint* gr-qc/9910076)
- [55] Shiromizu T and Ida D 2001 *Phys. Rev.* **D64** 044015 (*Preprint* hep-th/0102035)
- [56] Meert P and da Rocha R 2021 *Nucl. Phys. B* **967** 115420 (*Preprint* 2006.02564)
- [57] Meert P and da Rocha R 2022 *Eur. Phys. J. C* **82** 175 (*Preprint* 2109.06289)
- [58] Cavalcanti R T, de Paiva R C and da Rocha R 2022 *Eur. Phys. J. Plus* **137** 1185 (*Preprint* 2203.08740)
- [59] Yang Y, Liu D, Övgün A, Long Z W and Xu Z 2023 *Phys. Rev. D* **107** 064042 (*Preprint* 2203.11551)
- [60] Li Z 2023 *Phys. Lett. B* **841** 137902 (*Preprint* 2212.08112)
- [61] Avalos R and Contreras E 2023 *Eur. Phys. J. C* **83** 155 (*Preprint* 2302.09148)
- [62] Al-Badawi A, Jha S K and Rahaman A 2024 *Eur. Phys. J. C* **84** 145
- [63] Parker L E and Toms D 2009 *Quantum Field Theory in Curved Spacetime: Quantized Field and Gravity* Cambridge Monographs on Mathematical Physics (Cambridge University Press) ISBN 978-0-521-87787-9, 978-0-521-87787-9, 978-0-511-60155-2
- [64] Kuntz I and da Rocha R 2019 *Eur. Phys. J. C* **79** 447 (*Preprint* 1903.10642)
- [65] Kuntz I and da Rocha R 2020 *Nucl. Phys. B* **961** 115265 (*Preprint* 1909.10121)
- [66] Sharif M and Majid A 2022 *Chin. J. Phys.* **80** 285–304 (*Preprint* 2307.08005)
- [67] Tello-Ortiz F, Maurya S K and Gomez-Leyton Y 2020 *Eur. Phys. J. C* **80** 324
- [68] Maurya S K, Singh K N, Govender M and Ray S 2022 *Mon. Not. Roy. Astron. Soc.* **519** 4303–4324
- [69] de Freitas J a M L and Kuntz I 2023 (*Preprint* 2307.13803)
- [70] Kontsevich M and Segal G 2021 *Quart. J. Math. Oxford Ser.* **72** 673–699 (*Preprint* 2105.10161)
- [71] Unz R K 1986 *Nuovo Cim. A* **92** 397–426
- [72] Toms D J 1987 *Phys. Rev. D* **35** 3796
- [73] Moretti V 1997 *Phys. Rev. D* **56** 7797–7819 (*Preprint* hep-th/9705060)
- [74] Hatsuda M, van Nieuwenhuizen P, Troost W and Van Proeyen A 1990 *Nucl. Phys. B* **335** 166–196
- [75] van Nieuwenhuizen P 1990 *Nucl. Phys. B Proc. Suppl.* **16** 605–607
- [76] Armendariz-Picon C, Neelakanta J T and Penco R 2015 *JCAP* **01** 035 (*Preprint* 1411.0036)
- [77] Becker M and Reuter M 2020 *Phys. Rev. D* **102** 125001 (*Preprint* 2008.09430)
- [78] Buchbinder I L and Lyakhovich S L 1987 *Class. Quant. Grav.* **4** 1487–1501
- [79] Hamamoto S and Nakamura M 2000 *Prog. Theor. Phys.* **104** 691–702 (*Preprint* hep-th/0005131)
- [80] 't Hooft G and Veltman M J G 1972 *Nucl. Phys. B* **44** 189–213
- [81] Wilson K G 1975 *Rev. Mod. Phys.* **47** 773
- [82] Hossenfelder S 2013 *Living Rev. Rel.* **16** 2 (*Preprint* 1203.6191)
- [83] Casadio R and Kuntz I 2020 *Eur. Phys. J. C* **80** 958 (*Preprint* 2006.08450)
- [84] Casadio R, Feng W, Kuntz I and Scardigli F 2023 *Phys. Lett. B* **838** 137722 (*Preprint* 2210.12801)
- [85] Casadio R, Kamenshchik A and Kuntz I 2021 *Nucl. Phys. B* **971** 115496 (*Preprint* 2102.10688)

- [86] Kuntz I and da Rocha R 2023 *Nucl. Phys. B* **993** 116258 (*Preprint* 2211.11913)
- [87] DeWitt B S 2003 *Int. Ser. Monogr. Phys.* **114** 1–1042
- [88] Barvinsky A O and Vilkovisky G A 1987 *Nucl. Phys. B* **282** 163–188
- [89] Barvinsky A O and Vilkovisky G A 1985 *Phys. Rept.* **119** 1–74
- [90] Halliwell J J and Hartle J B 1990 *Phys. Rev. D* **41** 1815
- [91] Hartle J B and Hawking S W 1983 *Phys. Rev. D* **28** 2960–2975
- [92] Briscese F 2022 *Phys. Rev. D* **105** 126028 (*Preprint* 2206.09767)
- [93] Gibbons G W and Hawking S W 1977 *Phys. Rev. D* **15** 2752–2756
- [94] Gibbons G W, Hawking S W and Perry M J 1978 *Nucl. Phys. B* **138** 141–150
- [95] Louko J and Sorkin R D 1997 *Class. Quant. Grav.* **14** 179–204 (*Preprint* gr-qc/9511023)
- [96] Witten E 2021 (*Preprint* 2111.06514)
- [97] Lehnert J L 2022 *Phys. Rev. D* **105** 026022 (*Preprint* 2111.07816)
- [98] Chen Y 2022 *JHEP* **06** 137 (*Preprint* 2202.04741)
- [99] Visser M 2022 *JHEP* **08** 129 (*Preprint* 2111.14016)
- [100] Andriolo E, Lambert N, Orchard T and Papageorgakis C 2022 *JHEP* **04** 115 (*Preprint* 2112.00040)
- [101] Chapman S, Galante D A, Harris E, Sheorey S U and Vegh D 2023 *JHEP* **03** 006 (*Preprint* 2212.01398)
- [102] Ovalle J, Gergely L and Casadio R 2015 *Class. Quant. Grav.* **32** 045015 (*Preprint* 1405.0252)
- [103] Ovalle J and Linares F 2013 *Phys. Rev.* **D88** 104026 (*Preprint* 1311.1844)
- [104] Ivanov B V 2002 *Phys. Rev. D* **65** 104011 (*Preprint* gr-qc/0201090)